International Journal of Scientific Research and Engineering Development-– Volume 2 Issue 2, Mar – Apr 2019

Available at www.ijsred.com

RESEARCH ARTICLE OPEN ACCESS

Detection of Human Heart Rate and Respiratory Rate Using Thermal Infrared Image

D. Malathi[1], A.Mathangopi[2], Dr.D.RajiniGirinath[3],
[1]P.G Student,[2]Asst.Prof,[3]HOD,Department of CSE,
Sri Muthukumaran Institute Of Technology, Chikkarayapuram, Chennai,
Tamil Nadu-600069, India.

Abstract:

To achieve the simultaneous and unobtrusive breathing rate (BR) and heart rate (HR) measurements a far-infrared imager and an infrared camera equipped with IR-Cut lens and an infrared lighting array to develop a dual-camera imaging system.Heart rate is an important indicator for the mental and physical state, but it is usually measured through physical contact. In this paper a method introduced,where by measuring variations in color of reflected light, i.e., Hue, and can therefore measure both HR and respiratory rate (RR) from the image of a subject's face.The HR and respiratory signals measured remotely by using a Kinect sensor with a detection range of 3 meters. The overall performance of the proposed technique is acceptable for BR and HR estimations during nighttime.

Index Terms—**Heart rate, infrared sequence images, wavelet transform, thermal imaging, diagnostic imaging.**

I. INTRODUCTION

Heart rate monitoring is important in health care and affective computing. The conventional ways for heart rate measurement are electrocardiography (ECG) and photoplethysmography (PPG). Both methods need contact sensors, thus measurement itself may be a mental or physical stressor. Therefore, a mentally and physically low-restrictionmeasurement for the heart rate is highly desirable.It may be an external uncomfortable condition (heat, cold, etc.), or due to internal demands of the body.

As infrared thermography could detect tiny changes in the skin temperature due to the pulsation, it has also been used in heart rate measurement. The capability of custom-made infrared imaging system for monitoring had been also studied. A CMOS camera coupled with an infrared light operating at wavelength of 825 nm was applied for detecting the movement pattern [8]. Martinez and Stiefelhagen captured the fixed infrared dot matrix, and subsequently, the BR was estimated from the displacements of some dots caused by chest movements [9]. Apart from the methods based on movement detection, the variations of pixel intensities are also widely used signals to be served as some disorder symptoms. Thermal imaging technique can detect the radiation emitted by the objects whose temperature exceeds absolute zero, and therefore, it is very suitable for executing the tasks such as monitoring. The thermal imagery was employed to extract the temperature variations around the nostril regions [10].

The main contributions of this paper are to present: (1) a dual-camera setup that can carry out the simultaneous and unobtrusive BR and HR measurements; (2) a collaborative image processing method to detect and track the region of interest (ROI) as well as register images; and (3) a novel signal extraction method in time domain to accurately determine BR and HR.

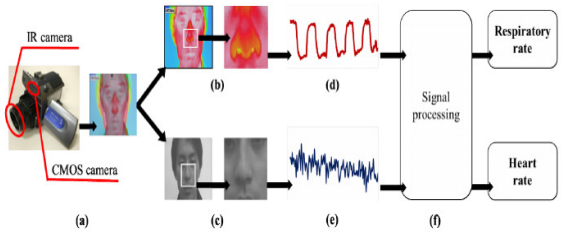

Fig. 1 Overview of thermal/RGB image processing method for calculating respiratory and heart rates. (a) A CMOS sensor camera and an IR camera integrated type thermography, which provides the thermal/RGB image-fusion mode. (b) The thermal image and its region of interest (ROI). (c) The RGB image and its ROI. (d) A respiratory waveform created from the differences of RGB values on each ROI images in time series. Each difference was calculated by subtracting the RGB pixel values of an image from those values of the next frame. (e) A heartbeat waveform created from the mean brightness of the green plane signals. (f) Signal processing concluding band-pass filter, normalization, and autocorrelation function.

II. MATERIALS AND METHODS

A. *Principle*

The disadvantage compared to the infrared image is that, due to few geometric and textural facial details, the thermal image is at present inadequate to design fast and reliable face detection algorithms [17]. Therefore, in the current work, the infrared image is used to assist in automatically recognizing face and facial tissue in thermal image. For BR, the principle of thermal imager is based on the fact that the temperature around the nose and mouth fluctuates throughout the inspiration and expiration cycle. In terms of HR, we can catch the subtle color variations caused by blood circulation from thermal video. However, these two targeted signals are mixed together in the raw extracted signal. Luckily, the common BR and HR are between 10–40 bpm and 60–100 bpm, respectively [18, 19]. As shown in Fig 1,there is no overlap for these two vital physiological indicators in the Fourier power spectrum, thus enabling the BR and HR to be measured simultaneously.

B. *Real-time thermal/RGB Image Processing for Non-contact Vital-sign Measurement:*

The thermal/RGB images were acquired and analyzed in LabVIEW (National Instruments, Austin, Texas, USA) with an IMAQ vision toolbox in real time. Fig. 2 provides an overview of the method to calculate the respiratory and heart rates. In this study, we used the CMOS-IR camera (Nippon Avionics, TVS-500EXLV, Japan), which was the same type used at the quarantine station of Narita International Airport in Japan [7]. As shown in Fig. 2-a, the TVS-500EXLV integrates a CMOS sensor camera and an IR camera, and provides the thermal and RGB image-fusion mode. The ratio of overlapped thermal andRGB images is adjustable. The thermal/RGB mixed-images were obtained at 30 frames per sec with a 640 × 480 pixel solution; each image is transmitted to PC via an image capture unit (Princeton, PCA-DAV2, Japan).

To calculate the respiratory rates, we focused on the first image of thermal-predominant images shown in Fig. 2-b. We manually set the region of interest (ROI, the pixel solution was approximately 150 × 150 pixels) to be the center of the subject's nasal area. While breathing, the ambient air in and out through the nose varied the temperature in the ROI. Therefore, each pixel value of red, green, and blue planes of thermal image in the ROI shows the variation along with breathing. We calculated the differences in pixel values of red,

green, and blue planes of each thermal image. Subsequently, the respiratory waveform was created from the differences of RGB values on each ROI image in a time series (Fig. 2-d). Each difference of RGB pixel value was calculated by subtracting the RGB pixel values of an image from the values of the next frame. The waveform was transmitted to the signal processing part (Fig. 2-f), applied to a digital band-pass filter (0.17– 0.42 Hz), and then normalized. After this process, we created the waveform of the autocorrelation function from the normalized waveform and calculated the respiratory rate from the peak-to-peak time interval.

C. Dual-camera imaging system

A thermal imager (MAG62, Magnity Electronics Co.Ltd., Shanghai, PR China) with the resolution of 640×480 and the pixel pitch of 17 μm is fixed on a tripod to prevent vibration during the experiments. Its spectral range and thermal sensitivity are 7.5–14 μm and 0.5˚C, respectively. An infrared camera with the resolution of 640×480 is stabilized on the top of the thermal imager. These two cameras are parallel to each other in such a way that the field of view is almost the same. A USB and patch cables are applied for infrared and thermal cameras to connect a computer, respectively. A custom-built image acquisition software is developed for the generation of two trigger signals, thereby allowing the simultaneous acquisition of thermal and infrared videos. The obtained videos are afterwards loaded into the Matlab R2014a for further analysis.

III. Results

A. BR measurement

The scatter plot and linear regression result of reference and measured BR. All scatter points located between the 95% upper and lower confidence intervals, and most of them were close to the line of perfect match, whose slope was equal to 1. From linear correlation analysis, the estimated BR was found to be relevant to the simultaneously-acquired reference BR with the determination coefficient (R2) of 0.831. The above results indicated that our approach was acceptable for BR measurement.

Each segment of the respiration signals was smoothed every 0.5 second after it passed the band-pass filter. After the smoothing, the short-term fluctuations were removed. The local maxima and minima of the respiration signal will purely represent the exhaling and inhaling peaks of the body, respectively.

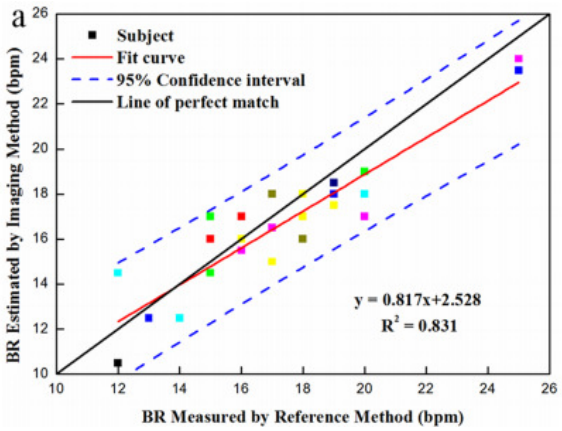

Fig:2 correlation between measured and reference BR

To make every signal segment (300s long in time) correspond to the effective arousal and be the same length, a 60s sub-segment was selected from every segment. For the baseline and relaxation test, the sub-segment was selected from 101s-200s of every segment, considering that the participant had adapted to the environment and may not be affected by the following stress test during this period. For the psychological stress, the sub-segment was selected from 201s-300s, considering that

psychological stress should have effect on the participant during this period. For the physical stress test, the sub-segment was selected from the 21s-120s, considering that subjects' breathing has been relatively smooth, and the effect of physical stress was strong during this period.

B. HR measurement

In respect to HR measurement, the scatter plot and regression line are presented. Apart from the one black point, the other testing data fell on the region between the two 95% confidence intervals. The strong correlation viz., R2 = 0.933 was observed between the measured and reference HRs, suggesting that the overall performance of the developed system is good for HR estimation. Although our system was to great extent robust against the low illumination, some unknown factors from experimental setup and environment would still influence.

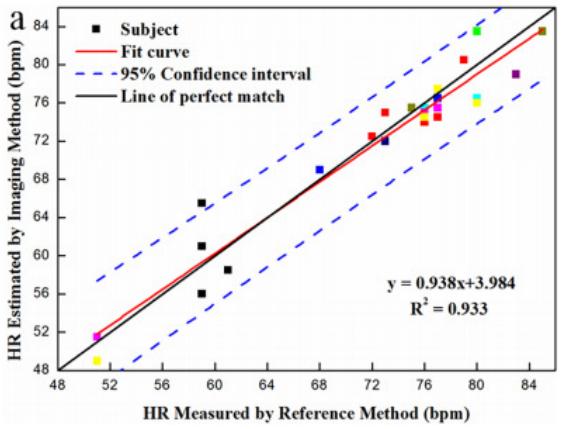

Fig:3 Correlation between measured and reference HR

All the features extracted under the baseline test were subtracted from the features extracted under the stress tests and relaxation test to avoid the effect of individual difference. Then, student's t-test were employed to select the useful features. A feature under three test, i.e., relaxation test, psychological stress test, and physical stress test, can produce three vectors. The feature will be regarded as useful if the t-test between any two vectors gives significant difference ($p<0.05$).

C. Detection and classification

After feature selection and dimensionality reduction, three one-to-many fisher classifiers were used to classify the three states, i.e., relaxation, psychological stress, and physical stress state. Each of them can distinguish one state from other states. Leave-One-Subject-Out method was used to verify the performance of these three fisher classifiers. It means that each time we use 29 participants' feature set as a training set, the remaining one participant's feature set as test set to test classifiers' classification performance. The test was repeated 30 times.

It is observed that the classification accuracy of three tests are all above 80%. The Psychological stress and physical stress can be recognized with 80% and 83% accuracy respectively. These results support that the stress can be recognized and that the psychological stress can be effectively discriminated from physical stress by using nocontact measured respiration signals.

IV. CONCLUSION AND DISCUSSION

We have presented a framework for detecting stress by using a Kinect sensor. The way of signal acquisition of Kinect characterizes the method a contact free stress detection method. The Kinect is small in size, light in

weight, and affordable to ordinary users, which make the method suitable for continuous monitoring of human stress in everyday life. The effect of physical stress when detecting psychological stress is considered in this research. When the context is unknown, the physical stress could be recognized as the psychological stress. By using features extracting from the respiration signal, we showed that the psychological stress can be differentiated from the physical stress.

REFERENCES

[1]. K. Hong, P. Yuen, T. Chen, A. Tsitiridis, F. Kam, M. Richardson, D. James, W. Oxford, J. Piper, F. Thomas and S. Lightman, "Detection and classification of stress using thermal imaging technique," Proceedings of the SPIE, 7486, pp. 0I01-09, 9 2009.

[2]. K. H. Kim, S. W. Bang and S. R. Kim, "Emotion recognition system using short-term monitoring of physiological signals," Med.Biol. Eng. Comput., vol. 42, p. 419–427, 2004.

[3]. T. Chen, P. Yuen, M. Richardson, G. Liu and Z. She, "Detection of psychological stress using a hyperspectral imaging technique," IEEE Transactions on Affective Computing, vol. 5, no. 4, pp. 391-405, 2014.

[4]. J. Healey and R. Picard, "SmartCar: Detecting driver stress," in Proc. 15th Int. Conf. Pattern Recognit., 2000.

[5]. McDuff, S. Gontarek and R. Picard, "Remote Measurement of Cognitive Stress via Heart Rate Variability," in 36th Annual International Conference of the IEEE on Engineering in Medicine and Biology Society , 2014.

[6]. U. Lundber, M. Forsman, G. Zachau, M. Eklof, G. Palmer, B. Melin and R. Kadefors, "Effects of experimentally induced mental and physical stress on motor unit recruitment in the trapezius muscle," Work and Stress, vol. 16, no. 2, pp. 166-178, 2002.

[7]. T. Chen, P. Yuen, K. Hong, A. Tsitiridis, F. Kam, J. Jackman, D. James, M. Richardson, W. Oxford, J. Piper, F. Thomas and S. Lightman, "Remote sensing of stress using electro-optics imaging technique," Proc. SPIE 7486, Optics and Photonics for Counterterrorism and Crime Fighting V, 748606, 9 2009.

[8]. T. Chen, P. Yuen, M. Richardson, G. Liu and Z. She, "Detection of psychological stress using a hyperspectral imaging technique," IEEE Transactions on Affective Computing, vol. 5, no. 4, pp. 391-405, 2014

[9]. Pavlidis, J. Dowdall, N. Sun, C. Puri, J. Fei and M. Garbey, "Interacting with human physiology," Comput. Vis. Image Understanding, vol. 108, pp. 150-170, 2007

[10]. A.Boiten, N. H. Frijda and C. J. Wientjes, "Emotions and respiratory patterns: review and critical analysis," International Journal of Psychophysiology, vol. 17, no. 2, pp. 103-128, 1994

[11]. S. Bloch, M. Lemeignan and N. Aguilera-T, " Specific respiratory patterns distinguish among human basic emotions," International Journal of Psychophysiology, vol. 11, no. 2, pp. 141-154, 1991.

[12]. P. Philippot, G. Chapelle and S. Blairy, "Respiratory feedback in the generation of emotion," Cognition & Emotion, vol. 16, no. 5, pp. 605- 627, 2002.

[13]. EY. Ng, GJ. Kaw, and WM. Chang, “Analysis of IR thermal imager for mass blind fever screening”, Microvascular Research, vol. 68(2), pp. 104–109, 2004.

[14]. MF. Chiang, PW. Lin, LF. Lin, HY. Chiou, CW. Chien, SF. Chu, and WT. Chiu, “Mass screening of suspected febrile patients with remote-sensing infrared thermography: alarm temperature and optimal distance,” Journal of the Formosan Medical Association, vol. 107(12), pp. 937–944, 2008.

[15]. Sun, T. Matsui, Y. Hakozaki, and S. Abe, “An infectious disease/fever screening radar system which stratifies higher-risk patients within ten seconds using a neural network and the fuzzy grouping method,” Journal of Infection, vol. 70(3), pp. 230–236, 2015.

[16]. MZ. Poh, DJ. McDuff, RW. Picard, “Advanced in Noncontact, Multiparameter Physiological Measurements Using Webcam”, IEEE Transactions on Biomedical Engineering, vol. 58(37), pp. 7– 11, 2011.

[17]. SC. Pei and JJ. Ding, “Reversible integral color transform,” IEEE Transactions Image Process, vol. 16(6), pp. 1686–1691, 2007.

[18]. G. Wyszecki and WS. Stiles, “Color Science: Concepts and Methods, Quantitative Data and Formulae.” Wiley, 1982.

[19]. F. Zhao, M. Li, Y. Qian and J. Tsien, "Remote measurements of heart and respiration rates for telemedicine," PloS one, vol. 8, no. 10, p. e71384, 2013.

[20]. Y. S. Lee, P. N. Pathirana, C. L. Steinfort and T. Caelli, "Monitoring and analysis of respiratory patterns using microwave doppler radar," IEEE journal of translational engineering in health and medicine, vol. 2, pp. 1-12, 2014.

[21]. N. Bernacchia, L. Scalise, L. Casacanditella, I. Ercoli, P. Marchionni and E. P. Tomasini, "Non contact measurement of heart and respiration rates based on Kinect," in 2014 IEEE International Symposium on Medical Measurements and Applications (MeMeA), Lisboa, 2014.

[22]. H. Aoki, M. Miyazaki, H. Nakamura, R. Furukawa, R. Sagawa and H. Kawasaki, "Non-contact respiration measurement using structured light 3-d sensor," in 2012 Proceedings of SICE Annual Conference (SICE), Akita, 2012.

[23]. F. Tahavori, E. Adams, M. Dabbs, L. Aldridge, N. Liversidge, E. Donovan, T. Jordan, P. Evans and K. Wells, "Combining marker-less patient setup and respiratory motion monitoring using low cost 3D

camera technology," in Proc. SPIE 9415, Medical Imaging 2015, Orlando, 2015.

[24]. Y. S. Lee, P. N. Pathirana, R. J. Evans and C. L. Steinfort, "Noncontact detection and analysis of respiratory function using microwave Doppler radar," Journal of Sensors, vol. 2015, p. 548136, 2015.

[25]. Y.-M. Kuo, J.-S. Lee and P.-C. Chung, "A Visual Context-AwarenessBased Sleeping-Respiration Measurement System," IEEE Transactions on Information Technology in Biomedicine, vol. 14, no. 2, pp. 255-265, 2010.

